



Citation for published version:

Ramin, P, Brock, AL, Causanilles, A, Valverde-Pérez, B, Emke, E, de Voogt, P, Polesel, F & Plosz, BG 2017, 'Transformation and sorption of illicit drug biomarkers in sewer biofilm', *Environmental Science and Technology*, vol. 51, no. 18, pp. 10572-10584. <https://doi.org/10.1021/acs.est.6b06277>

DOI:

[10.1021/acs.est.6b06277](https://doi.org/10.1021/acs.est.6b06277)

Publication date:

2017

Document Version

Peer reviewed version

[Link to publication](#)

This document is the Accepted Manuscript version of a Published Work that appeared in final form in *Environmental Science and Technology*, copyright © American Chemical Society after peer review and technical editing by the publisher. To access the final edited and published work see <https://doi.org/10.1021/acs.est.6b06277>.

University of Bath

General rights

Copyright and moral rights for the publications made accessible in the public portal are retained by the authors and/or other copyright owners and it is a condition of accessing publications that users recognise and abide by the legal requirements associated with these rights.

Take down policy

If you believe that this document breaches copyright please contact us providing details, and we will remove access to the work immediately and investigate your claim.

1 Transformation and sorption of illicit drug 2 biomarkers in sewer biofilms

3 Pedram Ramin^{a,b,*}, Andreas Libonati Brock^a, Ana Causanilles^c, Borja
4 Valverde-Pérez^a, Erik Emke^c, Pim de Voogt^{c,d}, Fabio Polesel^a, Benedek Gy.
5 Plósz^{a,e,*}

6 ^aDepartment of Environmental Engineering, Technical University of Denmark
7 (DTU), Bygningstorvet, Bygning 115, 2800 Kgs. Lyngby, Denmark

8 ^bProcess and Systems Engineering Center (PROSYS), Department of Chemical
9 and Biochemical Engineering, Technical University of Denmark, Building
10 229, 2800 Kgs. Lyngby, Denmark

11 ^cKWR Watercycle Research Institute, P.O. Box 1072, 3430 BB Nieuwegein,
12 The Netherlands`1

13 ^dInstitute for Biodiversity and Ecosystem Dynamics, University of Amsterdam,
14 P.O. Box 94248, 1090 GE Amsterdam, The Netherlands

15 ^eDepartment of Chemical Engineering, University of Bath, Claverton Down,
16 Bath BA2 7AY,UK

17

18 **Corresponding authors: pear@kt.dtu.dk; b.g.plosz@bath.ac.uk*

19

20 Abstract

21 In-sewer transformation of drug biomarkers (excreted parent drugs and metab-
22 olites) can be influenced by the presence of biomass in suspended form as well
23 as attached to sewer walls (biofilms). Biofilms are likely the most abundant
24 and biologically active biomass fraction in sewers. In this study, 16 drug bi-
25 omarkers were selected, including the major human metabolites of
26 mephedrone, methadone, cocaine, heroin, codeine and tetrahydrocannabinol
27 (THC). Transformation and sorption of these substances were assessed in tar-
28 geted batch experiments using laboratory-scale biofilm reactors operated under
29 aerobic and anaerobic conditions. A one-dimensional model was developed to
30 simulate diffusive transport, abiotic and biotic transformation and partitioning

31 of drug biomarkers. Model calibration to experimental results allowed estimat-
32 ing transformation rate constants in sewer biofilms, which were compared to
33 those obtained using in-sewer suspended biomass.

34 Our results suggest that sewer biofilms can enhance the transformation of most
35 compounds. Through scenario simulations, we demonstrated that the estima-
36 tion of transformation rate constants in biofilm can be significantly biased if
37 the boundary layer thickness is not accurately estimated. This study comple-
38 ments our previous investigation on the transformation and sorption of drug
39 biomarkers in the presence of only suspended biomass in untreated sewage. A
40 better understanding of the role of sewer biofilms—also relative to the in-sewer
41 suspended solids—and improved prediction of associated fate processes can
42 lead to more accurate estimation of daily drug consumption in urban areas in
43 wastewater-based epidemiological assessments.

44 Introduction

45 Wastewater-based epidemiology (WBE) has emerged as a new paradigm to
46 monitor trends of community-wide drug use based on chemical analysis of uri-
47 nary drug biomarkers in raw sewage, typically in the influent of wastewater
48 treatment plants (WWTPs).^{1,2} Transport in upstream sewer pipelines is known
49 to influence the quality of untreated wastewater³, hence reliable estimations of
50 drug use based on observations in WWTP influents require consideration of
51 in-sewer transformations and sorption of biomarkers. A recent investigation⁴
52 in a full-scale pressurized sewer pipeline revealed significant elimination or
53 formation of pharmaceuticals (e.g. bezafibrate and sulfamethoxazole, respec-
54 tively).

55 The uncertainty introduced by neglecting in-sewer processes is often ignored⁵
56 among other sources of uncertainty in WBE studies.⁶ The *in-sample* stability
57 of drug biomarkers has been widely assessed^{7–10}, providing an indication of
58 biotransformation in raw wastewater. These studies prominently addressed the
59 reliability of analysis after sample collection, focusing e.g. on biomarker sta-
60 bility during composite sample collections, rather than refining back-calcu-
61 lation schemes by accounting for in-sewer transformations. However, due to dif-
62 ferences in operation and design of sewer systems, *in-sewer* stability of drugs
63 of abuse is not only compound-specific but also highly dependent upon the
64 catchment layout (e.g., size¹¹) and the hydraulic conditions in the pipelines.

65 Moreover, in-sewer fate processes are not limited to biotransformation in the
66 bulk phase and biofilms/sediments, but also include abiotic processes and par-
67 titioning of drug biomarkers to suspended and attached solids. Drug bi-
68 omarkers can be in-sewer transformation product of other human metabolites
69 and hence their concentration can be significantly influenced. When consider-
70 ing these challenges, chemical *stability* in terms of percentage removal effi-
71 ciency or correction factors (lumped factors that include excretion ratio, in-
72 sewer transformation etc.) cannot be a reliable source of information for the
73 estimation of drug load at the point of excretion.

74 Recently, transformation and sorption of several drug biomarkers in raw
75 wastewater in the presence of suspended biomass have been assessed using
76 targeted experiments and mechanistic modelling.¹² This previous study eluci-
77 dated the role of only one of the possible actors of in-sewer biochemical pro-
78 cesses, as biomass in sewer systems is present also in attached form. However,
79 limited evidence exists on the role of sewer biofilms. To date, only a few stud-
80 ies^{13,14} assessed removal kinetics in sewer biofilms, showing enhanced relative
81 removal efficiency of selected drug biomarkers (cocaine and 6-mono-acetyl-
82 morphine) as compared to raw wastewater. Nevertheless, a number of previ-
83 ously uninvestigated factors are likely to influence (the estimation of) biofilm-
84 mediated transformation rates, namely (i) sorption onto biofilm¹⁵, similarly to
85 suspended solids in untreated wastewater¹²; (ii) concurrent transformation and
86 formation from other biomarkers^{8,12,16,17}; (iii) abiotic degradation^{5,12}; (iv) pre-
87 vailing redox conditions (aerobic and anaerobic); and (v) diffusive transport
88 through boundary layer and in biofilm^{15,18}. While being typically neglected in
89 biotransformation studies with biofilms, The impact of (v) may be substantial
90 considering the structure and the thickness of sewer biofilms and the reduced
91 diffusivity of large organic molecules.¹⁹⁻²¹ This is especially important in pres-
92 surized sewers, where sewer biofilms are abundant in completely filled
93 pipes.^{3,22}

94 In this study, we sought to improve the existing understanding of the fate of
95 drug biomarkers in the presence of sewer biofilms by means of an experimental
96 and model-based assessment. This study was meant to complement our previ-
97 ous investigation¹² on the fate of drug biomarkers in untreated sewage, in the
98 presence of only suspended biomass. The objectives of our investigation were
99 thus: (i) to assess the transformation and sorption of 16 drug biomarkers in
100 sewer biofilms under aerobic and anaerobic conditions (using laboratory-scale
101 rotating biofilm reactors); (ii) to model the fate of selected drug biomarkers in
102 the biofilm by explicitly describing diffusive transport and reaction kinetics;

103 (iii) to estimate biofilm-mediated biotransformation kinetics for the selected
104 biomarkers, and to compare them with transformation kinetics by suspended
105 biomass in untreated wastewater.

106 **Materials and methods**

107 **Selection of trace organic biomarkers.** Six illicit drugs were selected based
108 on their high consumption levels according to a recent European report.²³ The
109 target list was completed with 10 human metabolites and included: (i)
110 mephedrone (MEPH); (ii) methadone (METD) and its metabolite 2-ethylidene-
111 1,5-dimethyl-3,3-diphenylpyrrolidine (EDDP); (iii) cocaine (COC) and its me-
112 tabolites benzoylecgonine (BE), ecgonine methyl ester (EME), and co-
113 caethylene (CE); (iv) heroin (HER) and its metabolites 6-monoacetylmorphine
114 (6-MAM), morphine (MOR), and morphine-3- β -D-glucuronide (MORG); co-
115 deine (COE) and its metabolite norcodeine (NCOE); (v) tetrahydrocannabinol
116 (THC) and its metabolites 11-hydroxy- Δ^9 -THC (THCOH), and 11-nor-9-car-
117 boxy- Δ^9 -THC (THCCOOH). COE and NCOE were also considered in the
118 same group as MOR, since COE can potentially transform to MOR and NCOE
119 during human metabolism.²⁴ Analytical Standards (IS) and isotopically labeled
120 internal standard (ILIS) analogues from Sigma Aldrich (Brøndby, Denmark)
121 were dissolved in methanol or acetonitrile at concentrations of 0.1 mg mL⁻¹
122 and 1 mg mL⁻¹, respectively. Poor data quality prevented us from assessing the
123 transformation of methamphetamine and amphetamine, which are widely used
124 in Europe.²³

125 **Experimental set-up with continuous-flow operation.** Two annular rotating
126 biofilm reactors, made of poly(methyl methacrylate) (Plexiglas), operated ei-
127 ther under aerobic or anaerobic conditions with operating volume of 0.961 L,
128 were used to simulate in-sewer conditions by controlling, e.g., shear conditions
129 on biofilm. The reactors consisted of an inner rotating drum (diameter=9.0 cm)
130 and an outer stationary cylinder (diameter=11.4 cm), supporting the growth of
131 attached biomass. This type of reactor provided for high surface area to volume
132 ratio (175 m² m⁻³) that could be advantageous for biofilm growth. Each reactor
133 was equipped with four removable slides, allowing for inspection of biofilm
134 during reactor operation.

135 In order to establish stable aerobic and anaerobic biofilms, the two reactors were
136 operated under continuous-flow conditions for more than 7 months while being
137 kept in the dark. The rotation speed of the reactors was set to 20 rpm. The wall
138 shear stress was calculated according to equations provided by Rochex et al.²⁵ as

139 0.05 Pa which is in the lower range of typical wall shear stress in the sewers, meas-
140 ured up to 3 Pa in a gravity sewer.²⁶ Low shear stress was chosen in order to de-
141 crease biofilm sloughing and therefore enhance biofilm thickness. The reactors
142 were continuously fed (4 L d⁻¹, hydraulic residence time of approximately 0.25
143 d⁻¹) with pre-clarified wastewater from external cooled containers (T ≤ 4°C)
144 that were sparged with dry compressed atmospheric air (aerobic reactor) or
145 nitrogen (anaerobic reactor). The experiments were performed to mimic com-
146 pletely aerobic and anaerobic redox conditions. The external tanks were filled with
147 pre-clarified wastewater collected from Mølleåværket WWTP (Lundtofte, Den-
148 mark) semi-weekly. The wastewater had following characteristics: soluble organic
149 carbon, expressed as chemical oxygen demand (COD) = 40–130 g m⁻³, total COD
150 (120–g m⁻³), biological oxygen demand (BOD) = 90–200 g m⁻³, nitrate < 1 gN m⁻³,
151 total nitrogen (TN) = 20–50 gN m⁻³, sulfate = 12–55 gS m⁻³.

152

153 **Laboratory-scale batch experiments.** Following long-term continuous-flow
154 operation, two sets of batch experiments were performed: (i) biotransformation
155 experiments with intact biofilm in rotating reactors (BT); and (ii) sorption ex-
156 periments with re-suspended biofilm (SO). All experiments were started (t=0)
157 three minutes after spiking of biomarker standard solutions to ensure mixing
158 of spiked biomarkers in solution. Figure 1 illustrates the reactor configuration
159 and operation during BT Experiments. During the entire operation, the biofilm
160 reactors were kept full and intermittent wetting was avoided to prevent reduc-
161 tion of the overall activity of the biofilm. A detailed description of each set of
162 batch experiments is provided below. Description of all batch experiments is
163 also presented in SI Table S2.

164 *Biotransformation experiments (BT).* Each rotating biofilm reactor was con-
165 nected to an external container with a recirculating flow of 4 L h⁻¹. This con-
166 figuration allowed for sample collection from the external container without
167 changing the operating volume of the biofilm reactors. Two procedures were
168 considered. The first procedure (BT-P1) was conducted by spiking a mixture
169 containing all IS to obtain an initial (t=0) concentration of 10 µg L⁻¹. Following
170 sample withdrawal during experiments, samples were immediately spiked with
171 a mixture containing ILIS. The IS solution mixture contained the main target
172 compounds and ILIS were used to evaluate the analytical procedure. The sec-
173 ond procedure (BT-P2) was conducted by spiking ILIS at initial (t=0) concen-
174 tration of 2 µg L⁻¹. In this second case only ILIS were spiked and considered
175 the target compounds, including only MEPH-d3, METD-d3, EDDP-d3, COC-
176 d3, BE-d3, EME-d3, CE-d3, HER-d9 and 6MAM-d3. This procedure allowed

177 for the improved determination of illicit drug analytes without interference of
178 background concentrations (SI, Figure S3).¹³

179 The duration of the experiments was two days, during which 9 samples for BT-
180 P1 and 12 samples for BT-P2 experiments were collected (around 260 mL sam-
181 ple volume, see SI, Figure S2). During BT-P1 experiments, additional samples
182 were collected (i) before biomarker spiking, to measure the background con-
183 centrations; and (ii) during experiments, to monitor the biological activity of
184 the biofilms via measurements of chemical oxygen demand (COD), sulfate
185 ($\text{SO}_4\text{-S}$), ammonium ($\text{NH}_4\text{-N}$) and nitrate ($\text{NO}_3\text{-N}$).

186 BT-P1 and BT-P2 experiments were conducted after continuous-flow opera-
187 tion of biofilm reactors for 14 and 7 months, respectively assuming biofilm
188 reached maximum thickness. In this study, results of BT-P1 and BT-P2 exper-
189 iments were used for model identification/calibration (i.e., estimation of ki-
190 netic parameters and identification of transformation pathways) and for model
191 evaluation, respectively. For BT-P1 experiments (aerobic: $\text{pH}=8.7\pm 0.1$,
192 $T=17\pm 0.3$ °C; anaerobic: $\text{pH}=9.2\pm 0.4$, $T=17.8\pm 0.5$ °C), and BT-P2 experi-
193 ments (aerobic: $\text{pH}=8.8\pm 0.06$, $T=17.6\pm 0.2$ °C; anaerobic: $\text{pH}=8.7\pm 0.2$,
194 $T=17.5\pm 0.4$ °C), wastewater was collected from Mølleåværket WWTP
195 (Lundtofte, Denmark). Collected pre-clarified wastewater was centrifuged (20
196 min, 4700 rpm) and vacuum filtered (Advantec MFS, Inc., GA-55 grade) for
197 removal of suspended solids.

198 *Sorption experiments (SO)*. Sorption experiments (SO) were performed with
199 suspended aerobic biofilms (SO1) and suspended anaerobic biofilms (SO2).
200 The experiments were conducted after 14 months of continuous-flow operation
201 of the biofilm reactors. Tap water was circulated through the biofilm reactors
202 for 17 h to wash-off already sorbed compounds in the biofilm. Two slides were
203 removed from each reactor and intact biofilm was suspended in 2 L tap water
204 for 4 h for further desorption. After centrifugation (30 min, 4700 rpm), the
205 separated solids were mixed with 4 L vacuum filtered (Advantec MFS, Inc.,
206 GA-55 grade, pore size 6 μm) wastewater effluent (Mølleåværket WWTP,
207 Lundtofte, Denmark). To inactivate biomass during experiment, sodium azide
208 (0.05% v/v) was added to the mixture. The experiments were conducted for 4
209 h after spiking standard mixture and in total six samples (260 mL) were with-
210 drawn. During SO1 experiment ($\text{pH}=7.9\pm 0.1$, $T=15.4\pm 0.2$ °C) and SO2 exper-
211 iment ($\text{pH}=7.9\pm 0.1$, $T=15.3\pm 0.1$ °C), the reactors were sparged with dried com-
212 pressed air and nitrogen, respectively.

213 **Biofilm characterization.** The biofilm thickness (aerobic: 0.75 mm; anaero-
214 bic: 1.02 mm) was calculated by measuring biofilm volume and considering
215 the reactor surface area of 1679 cm². The biofilm volume was measured by
216 filling the rotating reactors with tap water without and with biofilm inside the
217 reactors. The difference between the volume of the empty reactor without bio-
218 film (961 cm³) and the free volume of the reactors with biofilm (aerobic reac-
219 tor, 836 cm³; anaerobic reactor, 790 cm³) was considered as the wet biofilm
220 volume. The solids content of the biofilm was measured by re-suspending the
221 biofilm on two removable slides into tap water, and subsequently measuring
222 total suspended solids (TSS) and volatile suspended solid (VSS) of the mixture.
223 The total dried mass per biofilm volume in the reactors, defined as biofilm
224 density, was then calculated (aerobic reactor, 55 gTSS L⁻¹, 22 gVSS⁻¹ L⁻¹; an-
225 anaerobic reactor, 83 gTSS L⁻¹, 38 gVSS⁻¹ L⁻¹).

226 **Sample preparation and chemical analyses.** Total suspended solids (TSS)
227 were measured using gravimetric analysis after filtration (0.6 µm glass fiber
228 filter, Advantec, USA).²⁷ Total and soluble COD, nitrate, ammonium and sul-
229 fate were measured using colorimetric methods (Hach Lange and Merck, Ger-
230 many). For dissolved components, the analyses were carried out after sample
231 filtration (0.45 µm cellulose acetate filters, Sartorius, Germany) and storage at
232 -20 °C.

233 For the analysis of drug biomarkers (one sample at each sampling time), a de-
234 scription of sample preparation and chemical analysis by liquid chromatog-
235 raphy coupled to high resolution mass spectrometry (HPLC-LTQ-Orbitrap)
236 can be found elsewhere.^{12,28} Briefly, samples were collected and immediately
237 frozen until analysis. For samples from SO experiments samples were first fil-
238 tered (0.6 µm glass fiber filter, Advantec, USA) to reduce the contact time
239 between solids and liquid phase. Later, samples were thawed and homoge-
240 nized, and 100 mL aliquots were extracted by solid phase extraction with Oasis
241 HLB cartridges (150 mg, 6 cc, Waters, Denmark). Extracts were reconstituted
242 in water:methanol (90:10, v/v) and 20 µL were injected into the HPLC-LTQ-
243 Orbitrap. Separation of the target compounds was achieved in an XBridge C18
244 column (150 mm × 2.1 mm, I.D., particle size 3.5 µm; Waters) with a MiliQ
245 and MeOH optimized gradient (each with 0.05% formic acid). Full scan accu-
246 rate mass data were acquired in positive electrospray ionization mode over a
247 m/z range of 50–600 Da at a resolution of 30000 full width at half maximum.
248 For confirmation purposes, information about the fragmentation spectra of the
249 target compounds was obtained by product-ion scan mode of the target masses

250 inclusion list, in the same analysis. All data were acquired and processed using
251 Xcalibur version 2.1 software.

252 **Modeling framework.** The mathematical description of fate processes was
253 formulated by accounting for temporal and spatial variation of target analyte
254 concentrations in biofilms. Due to mass transfer limitation from the bulk phase
255 to the biofilm and within the biofilm, concentration gradients can occur in the
256 biofilm reactors. For the specific case of batch experiments, it was assumed
257 that the biofilm is at steady state and as a homogeneous biomass. The volume
258 inside the biofilm reactors was constant, whereas in the external tank the vol-
259 ume decreased due to withdrawal of samples. Thus, the contact time between
260 the dissolved compounds in liquid phase and biofilm increased, which could
261 potentially enhance biomarker transformation. Consequently, residence time
262 dynamics were also included in the model by accounting for volume changes
263 in the external tank (SI Figure S2). As illustrated in Figure 1, the experimental
264 system consists of three compartments: (i) the bulk liquid in the rotating reac-
265 tor, (ii) the biofilm in the rotating reactor and (iii) the external tank (continu-
266 ously stirred tank reactor) connected to the biofilm reactor via a peristaltic
267 pump. The differential equations describing mass balances in each compart-
268 ment can be formulated as follows (all model parameters and state variables
269 are listed in Table 1):

270 i) In the biofilm reactor bulk phase:

$$271 \frac{dV_R C_{R,i}}{dt} = Q_{in,R} C_{in,R,i} - Q_{out,R} C_{R,i} - j_b A_b + r_{R,i} V_R \quad (\text{eq. 1})$$

272 ii) In the biofilm:

$$273 \frac{\partial V_b C_{b,i}}{\partial t} = A_b D \frac{\partial^2 C_{b,i}}{\partial z^2} \Delta z + r_{b,i} V_b \quad (\text{eq. 2})$$

274 iii) In the external tank:

$$275 \frac{dV_T C_{T,i}}{dt} = Q_{in,T} C_{in,T,i} - Q_{out,T} C_{T,i} + r_{T,i} V_T \quad (\text{eq. 3})$$

276 In these formulations, C (g m^{-3}) denotes the concentration as state variable and
277 the subscripts R , b and T indicate bulk phase of the rotating reactor, the biofilm,
278 and the external tank, respectively. The volume, which is constant for the re-
279 actor bulk phase V_R (m^{-3}) and the biofilm V_b (m^{-3}), changes as a function of
280 time inside the external tank, V_T (m^{-3}), as previously explained.

281 *Transport processes.* The flux of compounds between bulk phase and the bio-
282 film, j_b ($\text{g m}^{-2} \text{d}^{-1}$), is expressed using film theory at the mass transfer boundary
283 layer²⁹. The flux of compounds across the boundary layer can be defined as:

$$284 \quad j_b = k_b(C_R - C_L) = \frac{D}{L_b}(C_R - C_L) \quad (\text{eq. 4})$$

285 Where k_b (m d^{-1}) is the liquid-biofilm mass transfer coefficient, D ($\text{m}^2 \text{d}^{-1}$) is
286 the diffusion coefficient of the dissolved compounds into the biofilm, L_b (m) is
287 the biofilm thickness, and C_L is the concentration at the biofilm-liquid interface
288 (top layer). It was assumed that no reactions occur in the boundary layer. The
289 diffusion coefficients of target biomarkers in water, D_w ($\text{m}^2 \text{d}^{-1}$) were calculated
290 based on the revised Othmer-Thakar³⁰ equation suggested by Hayduk and
291 Laudie³¹:

$$292 \quad D_w = \frac{13.26 (10^{-5})}{\mu_w^{1.4} V_1^{0.589}}, \quad (\text{eq. 5})$$

293 where μ_w ($\text{kg m}^{-1} \text{s}^{-1}$) denotes the dynamic viscosity of water and V_1 ($\text{cm}^3 \text{g}$
294 mole^{-1}) is the molar volume of the substance. Diffusion coefficients (D_w) cal-
295 culated using eq. 5 are reported in Table S1. Diffusion coefficients inside the
296 biofilm were assumed to be reduced as compared to bulk water phase. Reduced
297 effective diffusivity results from limitation due to increased path length in bio-
298 film pores as compared to free aqueous media. Consequently, a dimensionless
299 effective diffusivity factor, f , was considered:

$$300 \quad D = fD_w \quad (\text{eq. 6})$$

301 The value of f was approximated by considering the density of the biofilm as
302 VSS (gVSS L^{-1}), based on the regression presented by Guimerà et al.³² The
303 boundary layer thickness, L_b , was estimated using dimensionless numbers,^{33,34}
304 namely Sherwood number (Sh), Schmidt number (Sc), Taylor number (Ta) and
305 Reynolds number (Re), (see SI, eqs. S1 to S4).

306 *Reaction processes.* Reaction kinetics in the bulk phase of the biofilm reactor
307 includes abiotic processes and biotransformation due to the presence of sus-
308 pended biomass. The amount of suspended solids was the residuals of solids
309 that remained in filtered wastewater (measured at $t=0$) and amount of detached
310 biomass assumed to be negligible. These processes were formulated according
311 to the Activated Sludge Model for Xenobiotics (ASM-X) framework.^{12,16} The
312 reaction rate for transformation of compound i and its formation from com-
313 pound j can be formulated as:

314 $r_{R,i} = -k_{abio}C_{R,i} + k_{abio}C_{R,j} \frac{M_i}{M_j} - \frac{k_{bio}X_{SS}}{(1+K_{d,i}X_{SS})}C_{R,i} + \frac{k_{bio}X_{SS}}{(1+K_{d,j}X_{SS})}C_{R,j} \frac{M_i}{M_j}$
 315 (eq. 7)

316 Where k_{abio} (d⁻¹) is the abiotic transformation rate, k_{bio} (L gTSS⁻¹ d⁻¹) is the
 317 TSS-normalized biotransformation rate constant for the suspended solids, K_d
 318 (L gTSS⁻¹) is the partitioning coefficient to suspended solids X_{SS} (g L⁻¹), and M
 319 is the molecular weight. Equilibrium processes were assumed for sorption and
 320 desorption onto suspended solids.

321 Inside the biofilm, in addition to abiotic processes, transformation and for-
 322 mation processes resulted from the microbial activity of the attached biomass.
 323 The associated kinetic equations were expressed as:

324 $r_{b,i} = -k_{abio}C_{R,i} + k_{abio}C_{R,j} \frac{M_i}{M_j} - k_{f,i}C_{b,i} + k_{f,j}C_{b,j} \frac{M_i}{M_j}$ (eq. 8)

325 $k_{f,j} = \frac{k_{biof,j}X_{SS}}{(1+K_{df,j}X_{SS})}$ (eq. 9)

326 In this formulation, biofilm-mediated transformation (subscript f) is expressed
 327 using pseudo-first order kinetics, where k_f and k_{biof} are in units of d⁻¹ and L
 328 gTSS⁻¹ d⁻¹, respectively, and K_{df} (L gTSS⁻¹ d⁻¹) is the partitioning coefficient in
 329 biofilms. Biofilm-mediated transformation can also be expressed by surface-
 330 normalized rate constants k'_{biof} (m³ m⁻² d⁻¹), obtained by dividing k_{biof} with
 331 $X_{SS} \cdot A_b/V_b$. The units of the reactions rates were adjusted to g m³ d⁻¹ according
 332 to the units in eq. 1-3.

333 Finally, the reaction kinetics in the external tanks were assumed to be the same
 334 as in the bulk aqueous phase of the biofilm reactor, with additional processes
 335 for sorption and desorption to and from the tank wall¹²:

336 $r_{T,i} = r_{R,i} - k_{des,w}k_{d,w}C_{T,i} \frac{A_T}{V_T} + k_{des,w}C_{Tw}$ (eq. 10)

337 Where C_{Tw} (g L⁻¹) denotes the biomarker concentration sorbed onto reactor
 338 wall, $K_{d,w}$ (m³ m⁻² d⁻¹) the partitioning coefficient to reactor wall. and $k_{des,w}$ (d⁻¹)
 339 is the desorption rate from the reactor wall.

340 **In-sewer transformation pathways.** Transformation and formation processes
 341 defined in eqs. 7–10 depend on the pathways identified for abiotic processes,
 342 transformation due to presence of suspended solids and biofilm-mediated
 343 transformations. The first two were adopted from our previous study.¹² Trans-
 344 formation pathways in biofilms were initially assumed based on reported hu-
 345 man metabolic pathways.^{7,35} This initial assumption was required due to the

346 absence of a priori evidence and was tested as part of the modelling study.
347 Subsequently, any deviation from the initial pathways was assessed by exam-
348 ining the mass balance over suggested transformed compounds and observed
349 transformation products (according to human metabolism).

350 **Model parameter estimation.** The values employed for k_{abio} and k_{bio} for sus-
351 pended biomass in bulk phase were estimated in an another study.¹² Using SO1
352 and SO2 measurements (SI, Figure S8) the K_{df} values were estimated accord-
353 ing to Ramin et al.¹² Values of k_f were estimated using the Bayesian optimiza-
354 tion method Differential Evolution Adaptive Metropolis (DREAM_(ZS)).³⁶ The
355 normalized sum of squared error (SSE) was used as objective function:

$$356 \quad SSE = \sum_{i=1}^n \sum_{j=1}^m \left(\frac{O_{i,j} - P_{i,j}}{O_{i,j,max} - O_{i,j,min}} \right)^2 \quad (\text{eq. 11})$$

357 Where n is the number of measurements series and m is the number of the data
358 points in each series. O denotes measured data, P model predictions, and $O_{i,j,max}$
359 and $O_{i,j,min}$ the maximum and minimum of measurements, respectively. To ad-
360 equately quantify the uncertainty associated to the k_f estimates, the uncertainty
361 from k_{abio} and k_{bio} was propagated according to the identified transformation
362 pathways for abiotic processes and biotransformation in presence of suspended
363 solids.³⁷ Values of k_{biof} were eventually estimated based on eq. 9. We consid-
364 ered an upper boundary threshold of 10^4 d^{-1} for k_f in parameter estimation. Pa-
365 rameter estimates beyond this threshold were considered to result from model
366 structure deficiencies (related to mass transfer).

367 **Model simulation and evaluation.** To simulate the transformation processes,
368 eqs. 1–3 were numerically solved following a spatial discretization of the bio-
369 film. Theoretically, increasing the discretization level (grid points) would in-
370 crease the accuracy of prediction at the expense of higher computational time.
371 For central grids (inside the biofilm), discretization was done using the central
372 difference formula. Values at the first grid (biofilm-liquid interface) and the
373 last grid points were computed via forward and backward difference, respec-
374 tively. This discretization scheme was adopted from the biofilm simulation
375 model developed by Vangsgaard et al.³⁸ The resulting set of ordinary differen-
376 tial equations was solved using the stiff ODE solver ode15s in Matlab R2014a
377 (MathWorks, US). Model parameter uncertainty was assessed using the poste-
378 rior probability distribution of estimates in Monte Carlo simulations as ex-
379 plained elsewhere.³⁹ Subsequently, the accuracy of the predictions was visually

380 evaluated comparing measurements from BT-P2 experiments, i.e. an independ-
381 ent dataset, with model predictions.

382 Results and discussion

383 **Biological activity of biofilm reactors.** To monitor microbial activity in aer-
384 obic and anaerobic biofilms, soluble COD, sulfate and ammonium (Figure 2)
385 as well as total COD and nitrate (SI, Figure S4) were monitored in the bulk
386 phase during the BT-P1 experiments (while reactors were disconnected from
387 continuous feeding). Soluble COD consisted of readily biodegradable organic
388 substrates and soluble inert fractions, including MeOH present in the spiking
389 solution. Utilization of MeOH as growth substrate was assumed to be negligi-
390 ble as in our previous study¹² we did not observe any substantial difference in
391 suspended biomass growth and oxygen uptake response upon MeOH addition.
392 Due to the likely higher activity of heterotrophic biomass under aerobic con-
393 ditions as well as higher MeOH evaporation rate (dried air was sparged at a
394 higher flow rate in the external tank compared to nitrogen gas), higher removal
395 of soluble COD was observed in the aerobic reactor (88%) compared to the
396 anaerobic one (57%) over 2 d. Due to the activity of sulfate reducing bacteria
397 (SRB), sulfate was significantly reduced under anaerobic conditions (62% over
398 1 d) and remained constant during last day of experiment (Figure 2b). This may
399 indicate that sulfate respiration by SRB species was limited by the absence of
400 readily biodegradable substrate during the second day of experiment. Under
401 aerobic conditions, the net formation (+33%) of sulfate was observed over 2 d,
402 possibly due to biochemical oxidation of hydrogen sulfide (H₂S) back to sul-
403 fate. In the aerobic BT-P1 reactor, ammonium removal is possibly dominated
404 by assimilatory ammonia uptake. It is also reported that nitrifiers are usually
405 overgrown by heterotrophic biomass in sewer biofilms (Huisman and Gujer,
406 2002; Jiang et al., 2009). Under anaerobic conditions, ammonium removal
407 could be due to assimilation and stripping – latter due to the comparably high
408 pH (9.2).

409

410 **Partitioning of drug biomarkers to biofilm.** Two solid-liquid partitioning
411 coefficients were estimated for aerobic ($K_{df,ae}$) and anaerobic biofilms ($K_{df,an}$)
412 using SO1 and SO2 experimental data, respectively (SI Figure S8). In addition,
413 abiotic chemical transformation was assessed in mineral water spiked with the
414 selected biomarkers – a study carried out previously.¹² These data were con-
415 sidered to disregard the contribution of abiotic transformation during sorption
416 experiments. Estimated partitioning coefficients are reported in SI Table S4.
417 The highest sorption capacity was found for THCOH ($K_{df,ae}=2.81$ L gTSS⁻¹;
418 $K_{df,an}=1.68$ L gTSS⁻¹). The drop in THC concentration in the sorption experi-
419 ments (72% in aerobic biofilms and 58% in anaerobic biofilm) can be inter-
420 preted as a result of chemical partitioning to external tank wall, as it was ob-
421 served previously¹², with the K_{df} values being negligible despite the high hy-
422 drophobicity of this chemical ($\log K_{ow}=7.6$).⁴⁰ However, given the high hydro-
423 phobicity of THC, high sorption onto biofilm solids could not be ruled out, and
424 further experimental confirmation may be required to verify our findings. Sorp-
425 tion of THCCOOH, EME and EDDP was only observed for anaerobic biofilms
426 ($K_{df,an}=1.06$ L gTSS⁻¹; 1.59 L gTSS⁻¹; $K_{df,an}=0.15$ L gTSS⁻¹ respectively). Con-
427 versely, partitioning under aerobic conditions was found for MEPH
428 ($K_{df,ae}=0.20$ L gTSS⁻¹). For the remaining chemicals, negligible sorption was
429 observed, hence K_{df} values were set to zero. Notably, the anaerobic biofilm had
430 higher thickness and density compared to the aerobic biofilm, which may ex-
431 plain the selective sorption of some of the drug biomarkers.

432 **Transformation of drug biomarkers.** Measurements from BT-P1 experi-
433 ments were used to calibrate developed 1-D model and to predict temporal and
434 spatial concentration profiles of drug biomarkers in the presence of sewer bio-
435 films. Biotransformation due to the presence of suspended solids was ac-
436 counted for by including previously estimated k_{bio} (L gTSS⁻¹ d⁻¹)^{12,37} (SI, Table
437 S3). Measured TSS concentrations in the bulk were considered constant,
438 namely, 42 mgTSS L⁻¹ and 104 mgTSS L⁻¹ (for BT-P1 aerobic and anaerobic,
439 respectively) 92 mgTSS L⁻¹ and 80 mgTSS L⁻¹ (for BT-P2 aerobic and anaero-
440 bic, respectively). The abiotic transformation rates k_{abio} and partitioning coef-
441 ficients of drug biomarkers to suspended solids, K_d (L gTSS⁻¹), were set at
442 values reported in SI, Table S3.¹² Subsequently, biofilm-mediated biotransfor-
443 mation rates k_f (d⁻¹) and rate constants k_{biof} (L gTSS⁻¹ d⁻¹) and k'_{biof} (m³ m⁻² d⁻¹)
444 were estimated.

445 Measured and simulated concentration profiles of all targeted biomarkers, ob-
446 tained through model calibration and validation, are presented in Figure 3. Ex-
447 perimental and simulation results describe removal and formation of selected

448 drug biomarkers in the bulk phase of the biofilm reactor, where samples were
449 collected. The simulation results obtained through model calibration are pre-
450 sented using the median of the estimated parameters (full and dash lines) with
451 the corresponding 95% credibility interval (shaded uncertainty band). The un-
452 certainty boundary ranges, shown in Figure 3, were obtained through the prop-
453 agation of the uncertainties from abiotic and biotic transformation rates (quan-
454 tified here or previously¹²) to the model outputs. The transformation pathways
455 identified in this study are presented in Figure S6–7. Parameter values esti-
456 mated (reported as median \pm credibility interval) are listed in Table S5 and all
457 posterior distributions of k_f values are given in Figure S11. Experimental and
458 modelling results are presented and discussed in detail for each group of chem-
459 icals in the following paragraphs.

460 Prior to estimating values of k_f , the impact of discretization number (i.e. the
461 number of layers in which the biofilm is discretized) on the prediction accuracy
462 was assessed. The case of the aerobic transformation rates for MEPH, $k_{f,ae,MEPH}$,
463 and HER, $k_{f,ae,HER}$, is discussed in detail (Figure 4, X-Z axis; Figure S5). HER
464 and MEPH were chosen because they represent compounds with low and high
465 removal rate, respectively. Discretization numbers, selected in the interval of
466 5-100 layers, were used to estimate k_f and using the highest level used to bench-
467 mark the level of error introduced by inaccurate model simulations. The dif-
468 ference is reported as relative percentage error, in which best-fit estimates for
469 $k_{f,ae,HER}$ and $k_{f,ae,MEPH}$ were compared with their corresponding reference values,
470 214.1 d⁻¹ and 24.3 d⁻¹, respectively. It was observed that the number of dis-
471 cretization had a different impact on the estimated k_f of these two chemicals,
472 and that after 80 grid points the resulting error was negligible (< 1 %) and
473 independent of the discretization number. This discretization number corre-
474 sponds to $\Delta Z=9.3 \mu\text{m}$ and $\Delta Z=12.8 \mu\text{m}$ for aerobic and anaerobic biofilms,
475 respectively.

476 *Mephedrone*. MEPH removal was more pronounced in the aerobic reactor
477 (77% versus 47% in the anaerobic reactor). Higher partitioning to aerobic bio-
478 films resulted in much higher biotransformation rate constants under aerobic
479 conditions ($k_{biof,ae,MEPH}=5.89 \text{ L gTSS}^{-1} \text{ d}^{-1}$, $k_{biof,an,MEPH}=0.08 \text{ L gTSS}^{-1} \text{ d}^{-1}$). The
480 comparably high sorption of MEPH in aerobic biofilms ($K_{df,ae}=0.2 \text{ L gTSS}^{-1}$)
481 makes this compound less bioavailable for microbial transformation. This im-
482 pact is also reflected in eq. 9, in which k_{biof} is in the numerator and K_{df} is in
483 denominator. Moreover, the higher aerobic k_{biof} obtained in this study agrees
484 well with those reported previously¹² ($k_{bio,ae,MEPH}=1.86 \text{ L gTSS}^{-1} \text{ d}^{-1}$,

485 $k_{bio,an,MEPH}=0$ L gTSS⁻¹ d⁻¹). The model could adequately simulate BT-P2 da-
486 taset under both redox conditions, thereby validating the process model struc-
487 ture identified.

488 *Methadone*. Since formation of EDDP after rapid removal of METD, especially
489 under aerobic conditions, was not observed (Fig. 3), these chemicals were consid-
490 ered to have independent pathways – similar to that obtained with suspended in-
491 sewer solids.¹² Our analyses showed rather small deviation between duplicates
492 (sample analysis), i.e. $\leq 7.5\%$ for METD and $\leq 4.5\%$ for EDDP.

493 Biotransformation of METD in sewer biofilms was found to be significantly
494 faster under aerobic conditions ($k_{biof,ae,METD}=2488$ L gTSS⁻¹ d⁻¹, $k_{biof,an,METD}=183$
495 L gTSS⁻¹ d⁻¹), which agrees well with data obtained with in-sewer suspended
496 solids.¹² Conversely, enhanced anaerobic transformation was observed for
497 EDDP ($k_{biof,ae,EDDP}=1.79$ L gTSS⁻¹ d⁻¹, $k_{biof,an,EDDP}=88.9$ L gTSS⁻¹ d⁻¹). Simula-
498 tion results (Fig. 3) for EDDP (both redox conditions) as well as for METD
499 (only anaerobic conditions) indicate a systematic deviation between the pre-
500 dicted and measured values. This may imply that the model structure should
501 be re-evaluated in future studies. A possible explanation could be related to
502 cometabolic effects, i.e. primary substrate oxidation can enhance secondary
503 substrate (i.e. drug biomarker) biotransformation.^{41–43} Additionally, under an-
504 anaerobic conditions, the sulfate remained constant after day 1 (Figure 2b). This
505 may suggest that readily biodegradable substrates were depleted during the
506 second day of experiment, resulting in negligible removal of EDDP and
507 METD. Nevertheless, simulations could not well predict the BT-P2 dataset es-
508 pecially for METD, in which lower removal was observed as compared to BT-
509 P1 measurements, as the process model do not account for cometabolic effects.

510 *Cocaine*. The transformation pathways for COC and its human metabolites
511 were selected based on Bisceglia et al.⁴⁴ Although the biotransformation of
512 COC to EME has been reported to be almost insignificant in raw wastewater
513 and activated sludge^{16,45}, in this study EME was considered as a transformation
514 product (Fig. S6d) of COC in sewer biofilms. Accordingly, it has been reported
515 that, in sewer biofilms, there should be another major transformation product
516 from COC other than BE as it was speculated previously.¹³ Net removal of
517 COC, CE and EME and net formation of BE was observed over the duration of
518 experiments, where BE formation resulted from hydrolysis of COC and CE.^{12,44}
519 Under aerobic conditions, the overall biotransformation rate constant of COC,
520 i.e. COC to BE and COC to EME, was lower than under anaerobic conditions
521 ($k_{biof,ae,COC}=0.44$ L gTSS⁻¹ d⁻¹, $k_{biof,an,COC}=2.57$ L gTSS⁻¹ d⁻¹). An even more
522 pronounced deviation was observed for EME ($k_{biof,ae,EME}=0.05$ L gTSS⁻¹ d⁻¹,

523 $k_{biof,an,EME}=21.03$ L gTSS⁻¹ d⁻¹), mainly due to the high biotransformation of
524 EME in the bulk phase under aerobic conditions, SI Table S3. Aerobic and
525 anaerobic percentage removal of COC only by sewer biofilms was found to be
526 3% and 33% larger than the removal observed in raw wastewater under corre-
527 sponding redox conditions.¹² In contrast, Thai et al.¹³ found 25% and 40% en-
528 hancement of COC removal in gravity sewer (aerobic/anaerobic) and rising
529 sewer (anaerobic) conditions, respectively compared to removal with
530 wastewater only. In our study, CE biotransformation kinetics obtained under
531 aerobic and anaerobic biofilms were comparable ($k_{biof,ae,CE}=0.68$ L gTSS⁻¹ d⁻¹,
532 $k_{biof,an,CE}=0.51$ L gTSS⁻¹ d⁻¹). BE is formed from COC and CE transformations
533 and also transformed to another unknown transformation product
534 ($k_{biof,ae,BE}=2.00$ L gTSS⁻¹ d⁻¹, $k_{biof,an,BE}=0.95$ L gTSS⁻¹ d⁻¹). Values of k'_{biof} (m³
535 m⁻² d⁻¹) estimated in this study (SI, Table S4) for overall COC, BE and CE for
536 aerobic biofilms ($k'_{biof,ae,COC}=0.13$ m³ m⁻² d⁻¹, $k'_{biof,ae,BE}=0.57$ m³ m⁻² d⁻¹,
537 $k'_{biof,ae,CE}=0.39$ m³ m⁻² d⁻¹) are almost 4 times, 34 and 2 times higher than the
538 values reported by McCall et al.¹⁴ (aerobic biofilms at 21°C). In contrary, for
539 BE, no transformation by in-sewer suspended solids and sewer biofilms was
540 reported.¹³ The differences are possibly due to different microbes residing in
541 the biofilms in these studies.

542 *Heroin*. Transformation of heroin biomarkers was assumed to follow the path-
543 ways previously described for human metabolism^{24,35,46}, namely two-step de-
544 acetylation to 6MAM and to MOR. MORG was also considered to be trans-
545 formed to MOR via deconjugation.⁴⁷ It was hypothesized that COE was not
546 only transformed to NCOE by sewer biofilms but also to MOR as it was ob-
547 served in raw wastewater under anaerobic conditions.³⁷ Nevertheless, biofilm-
548 mediated biotransformation processes could be described with transformation
549 pathways similar to human metabolism. HER was rapidly removed in both
550 sewer biofilms (similarly to raw wastewater (SI, Figure S9), with higher bio-
551 transformation kinetics in anaerobic biofilms ($k_{biof,ae,HER}=4.43$ L gTSS⁻¹ d⁻¹,
552 $k_{biof,an,HER}=22.14$ L gTSS⁻¹ d⁻¹). Likewise, a five-fold increase of 6MAM bio-
553 transformation kinetics was observed in anaerobic biofilms ($k_{biof,ae,6MAM}=1.11$
554 L gTSS⁻¹ d⁻¹, $k_{biof,an,6MAM}=6.45$ L gTSS⁻¹ d⁻¹). These differences cannot be ex-
555 plained only by considering differences in the removal of 6MAM in aerobic
556 and anaerobic biofilms (i.e. 33% and 59% in aerobic and anaerobic biofilms in
557 12 h experimental time (SI, Figure S9). Thus, additional processes are assumed
558 to be involved, notably, the formation of 6MAM from HER. Given that the
559 6MAM biotransformation by in-sewer suspended solids is significantly lower
560 than in biofilms, the total % removal is not substantially different from those

561 reported by Thai et al.¹³ However, McCall et al.¹⁴ found 3 times higher bio-
562 transformation rate for 6MAM by aerobic biofilm compared to in-sewer sus-
563 pended solids. In this study, as to pathway identification, no additional trans-
564 formation product of HER was considered when assessing the conservation of
565 HER mass. Moreover, MORG was found to be transformed only by anaerobic
566 sewer biofilm ($k_{biof,an,MORG}=2.03 \text{ L gTSS}^{-1} \text{ d}^{-1}$) – a rate approximately 6 times
567 lower than that by in-sewer suspended biomass.¹² Due to rapid aerobic trans-
568 formation of MORG in the bulk, no aerobic biofilm-induced removal was ob-
569 served for MORG. High transformation of MORG was also observed by Senta
570 et al.⁸ in wastewater.

571 Biotransformation rates obtained for COE and NOE in biofilms are at a mod-
572 erate level, with NCOE having higher transformation under anaerobic condi-
573 tions. The simulation model identified can effectively simulate the fate of HER
574 and 6-MAM transformation in the BT-P2 independent datasets, thereby vali-
575 dating the modelling approach.

576 *THC*. In untreated wastewater, THCOH was not found to be a transformation
577 product of THC.¹² Accordingly separate transformation pathways were as-
578 sumed for THC and THCOH in sewer biofilms. Based on pathways suggested
579 in literature,³⁵ THCCOOH was considered to be formed from THCOH.³⁵ As a
580 result of poor data quality, no clear conclusion could be drawn for THC bio-
581 transformation especially under anaerobic conditions. Moreover, the
582 $k_{biof,ae,THC}=0$ as THC removal was completely attributed to partitioning to the
583 external tank and abiotic hydrolysis. Hence, model calibration could not be
584 performed using THC data set (SI, Figure S10). THCOH exhibited comparably
585 high biotransformation rate constants ($k_{biof,ae,THCOH}=21034 \text{ L gTSS}^{-1} \text{ d}^{-1}$,
586 $k_{biof,an,THCOH}=5066 \text{ L gTSS}^{-1} \text{ d}^{-1}$), which were also observed for THCCOOH bi-
587 otransformation in the anaerobic biofilm ($k_{biof,an,THCCOOH}=3272 \text{ L gTSS}^{-1} \text{ d}^{-1}$).

588 We note that the high k_{biof} values corresponded to high K_{df} values for these
589 chemicals (SI Table S4), a factor that makes THCOH and THCCOOH less bi-
590 oavailable for biotransformation. Interestingly, aerobic THCCOOH biotrans-
591 formation obtained ($k_{biof,ae,THCCOOH}=133 \text{ L gTSS}^{-1} \text{ d}^{-1}$) was lower than that un-
592 der anaerobic conditions.

593 **The impact of mass transfer limitation.** Compared to common growth sub-
594 strates, illicit drug biomarkers are relatively large molecules. The average mo-
595 lar volume, V_l ($\text{cm}^3 \text{ mol}^{-1}$), of biomarkers in this study is $250 \text{ cm}^3 \text{ mol}^{-1}$, sig-
596 nificantly larger than the molar volume of readily biodegradable substrates

597 such as acetate (56.1 cm^{-3}).⁴⁸ Therefore, the comparably high molar volume is
598 assumed to significantly impact diffusivity of drug biomarkers in biofilm.

599 In general, the concentration in the boundary layer is proportional to the ratio
600 of convective mass transfer (i.e. axial flow in biofilm reactor) to diffusive mass
601 transport (Sh number). According to eq. 5, molecules with a higher molar vol-
602 ume and low diffusivity are expected to have lower boundary layers (SI Figure
603 S1). In biofilm modeling studies, typically an average boundary layer is as-
604 sumed for all chemicals, under the condition that this approximation does not
605 impact the accuracy of predictions; this, however, is generally done without
606 proper error assessment. Figure 4 (Y-Z axis) illustrates the impact of the choice
607 of boundary layer thickness on the accuracy of estimation of biotransformation
608 rate, k_f , for the example of MEPH and HER in aerobic biofilms. Estimated
609 values for a range of boundary layer thicknesses (5 to 100 μm) together with
610 discretization number (10 to 100) were compared with reference predictions
611 for MEPH (30 μm) and HER (20 μm) with discretization number of 100. These
612 results indicate that the impact of the boundary layer thickness on parameter
613 estimates (i) is compound-specific; and (ii) varies by the discretization number
614 employed (Figure 4 X-Z axis). A higher influence was observed for more re-
615 active compounds, i.e. HER, at lower discretization numbers. In Figure 4, red
616 dots denote the values employed in this study (discretization number=80 lay-
617 ers; boundary layer thickness=23 μm). Furthermore, diffusion of HER and
618 MEPH was compared in aerobic and anaerobic biofilms through simulation of
619 diffusive transport, considering negligible partitioning to solids and transfor-
620 mation (SI Figure S12). Following the spiking of internal standards in BT-P1
621 experiments, the concentrations in the bulk phase of the reactors were predicted
622 to reach an equilibrium level after 2 h in aerobic biofilms and 4 h in anaerobic
623 biofilms. These delays show the impact of mass transfer limitation across the
624 boundaries of biofilm and liquid phase – a factor that necessitates an effective
625 diffusion modelling for which we provided an example here. Moreover, the
626 recirculation between external tank and reactor cause additional limiting step
627 for reaching equilibrium. An example of concentration profile inside the bio-
628 film is also presented for MEPH (SI, Figure S13).

629 **Transformation in raw wastewater and sewer biofilms – A comparison.**

630 Biotransformation rate constants in sewer biofilms k_{biof} estimated in this study
631 were compared rate constants in the presence of suspended solids, k_{bio} (Figure
632 5).¹² Under aerobic conditions (reproducing a gravity sewer), most biomarkers
633 exhibited similar k_{biof} and k_{bio} values (see error bars in Figure 5). Biofilm-me-
634 diated transformations were found to be dominant for COE and NCOE, whilst

635 the majority of MORG and MOR transformation occurred in the bulk water by
636 suspended biomass. Under anaerobic conditions, MEPH, METD, COC, EME,
637 CE, THCOH, and THCCOOH were found to be biotransformed only in bio-
638 films. Moreover, no additional major transformation products for HER and
639 MORG, other than 6MAM and MOR, respectively, were identified in the bio-
640 film reactors, as opposed to raw wastewater.

641 **Future perspectives.** In this study, we assessed the transformation of 16 drug
642 biomarkers in biofilm reactors under aerobic and anaerobic conditions, repre-
643 senting typical conditions in gravity and pressure sewers (respectively). This
644 investigation complemented our previous study¹² on the fate of drug bi-
645 omarkers in raw sewage, in the presence of suspended biomass only. A com-
646 parative assessment of the results indicates that sewer biofilms enhance the
647 transformation kinetics of many of selected drug biomarkers, particularly un-
648 der anaerobic conditions (Figure 5), likely due to higher anaerobic activity in
649 biofilms than in suspended biomass. Under aerobic conditions, transformation
650 kinetics in biofilms was overall comparable to that observed for untreated
651 sewage, indicating again limited stability of selected biomarkers. This evi-
652 dence suggests the necessity of accounting for biofilm-mediated transfor-
653 mation when predicting in-sewer fate of drug biomarkers. Moreover, for the
654 reliable prediction of trace organic chemical fate in biofilm, the mathematical
655 consistency of simulation model structures should be assessed.

656 More observations are needed to validate sorption and transformation of THC
657 in sewer biofilms. In this study all drug biomarkers (parents and metabolites)
658 were spiked simultaneously to simulate environmentally-relevant conditions,
659 i.e. the occurrence of drug biomarkers in sewer as a mixture. The developed
660 model however could describe the transformations among biomarkers. Never-
661 theless, future experimental designs used could benefit from spiking unrelated
662 biomarkers (e.g., in separate batch experiments) or using biomarkers with sev-
663 eral different labels, although resulting in a drastic increase of the cost of chem-
664 ical analysis.

665 The microbial activity of the two biofilms in this study was characterized by
666 monitoring utilization of primary substrates (e.g., organic carbon, sulfate) dur-
667 ing batch experiments. Our results showed substantial differences in microbial
668 activity between the two biofilms assessed in this study, e.g., significantly
669 higher sulfate-reducing activity in the anaerobic biofilm. In sewer systems, mi-
670 crobrial functions and community of sewer biofilms vary over a sewer length
671 likely as a result of changes in boundary conditions and gradients in substrate

672 concentrations and wastewater composition. To date, this has been demon-
673 strated for gravity sewers¹⁴. Hence, further research is required to characterize
674 microbial activity of the sewer biofilms at different sewer locations and corre-
675 late the microbial community and activity with biotransformation rates.

676 In this study, the aeration was performed in a separate tank and not directly in
677 the biofilm reactor. The objective was to provide sufficient oxygen supply to
678 ensure that most microorganisms would be exposed to aerobic conditions. It
679 should be noted that (re)aeration may be different in full-scale sewer systems,
680 being caused by flow fluctuations and mixing. The current study potentially
681 offers the background for a combined modelling framework for real sewers,
682 where switching functions based on dissolved oxygen concentration would al-
683 low differentiating between aerobic and anaerobic conditions.

684 Although this study compared the biotransformation rate in raw wastewater
685 and in biofilms, the contribution of each of these biotransformation processes
686 to the overall drug biomarkers removal should be assessed. Moreover, the as-
687 sessment of drug abuse rates at catchment level should account for, im-
688 portantly, the layout of the sewer system, hydraulic conditions⁴⁹ and the possi-
689 ble drug release patterns. Additionally, model-based back-calculation tools
690 should account for abiotic processes and biotransformation induced by sus-
691 pended biomass and sewer biofilms.⁵⁰ Hence, a reactive-transport model needs
692 to be developed, describing drug biomarkers transformation under steady-state
693 and dynamic conditions. Transformation rates estimated in this study can be
694 used to calibrate such simulation models. Our ongoing research⁵⁰ is addressing
695 the impact of neglecting in-sewer biotransformation on estimation of daily
696 drug consumption in catchments using uncertainty analysis and measurements
697 from sampling campaigns. Results presented in this study underscore the high
698 level of complexity of in-sewer biomarker fate, of which the implications to
699 wastewater-based epidemiological engineering are numerous.

700 Acknowledgments

701 This study was supported by the European Union's Seventh Framework Pro-
702 gramme for research, technological development and demonstration [grant
703 agreement 317205, the SEWPROF MC ITN project]. Borja Valverde-Pérez
704 thanks the Technical University of Denmark (DTU) for the financial support
705 through the KAIST-DTU project on Integrated Water Technology (InWaTech,
706 <http://www.inwatech.org>).

707 Reference

- 708 (1) Thomas, K. V.; Bijlsma, L.; Castiglioni, S.; Covaci, A.; Emke, E.; Grabic, R.;
709 Hernández, F.; Karolak, S.; Kasprzyk-Hordern, B.; Lindberg, R. H.; et al. Comparing
710 illicit drug use in 19 European cities through sewage analysis. *Sci. Total Environ.*
711 **2012**, *432*, 432–439.
- 712 (2) Daughton CG. Illicit drugs in municipal sewage: proposed new non-intrusive tool to
713 heighten public awareness of societal use of illicit/abused drugs and their potential
714 for ecological consequences. In *American Chemical Society, Symposium Series*;
715 American Chemical Society, Symposium Series: Washington, DC, 2001; p 348–364.
- 716 (3) Hvitved-Jacobsen, T.; Vollertsen, J.; Matos, J. S. The sewer as a bioreactor - A dry
717 weather approach. *Water Sci. Technol.* **2002**, *45* (3), 11–24.
- 718 (4) Jelic, A.; Rodriguez-Mozaz, S.; Barceló, D.; Gutierrez, O. Impact of in-sewer
719 transformation on 43 pharmaceuticals in a pressurized sewer under anaerobic
720 conditions. *Water Res.* **2014**, *68*, 98–108.
- 721 (5) McCall, A.-K.; Bade, R.; Kinyua, J.; Lai, F. Y.; Thai, P. K.; Covaci, A.; Bijlsma, L.;
722 van Nuijs, A. L. N.; Ort, C. Critical review on the stability of illicit drugs in sewers
723 and wastewater samples. *Water Res.* **2016**, *88*, 933–947.
- 724 (6) Castiglioni, S.; Bijlsma, L.; Covaci, A.; Emke, E.; Hernández, F.; Reid, M.; Ort, C.;
725 Thomas, K. V.; Van Nuijs, A. L. N.; De Voogt, P.; et al. Evaluation of uncertainties
726 associated with the determination of community drug use through the measurement
727 of sewage drug biomarkers. *Environ. Sci. Technol.* **2013**, *47* (3), 1452–1460.
- 728 (7) van Nuijs, A. L. N.; Abdellati, K.; Bervoets, L.; Blust, R.; Jorens, P. G.; Neels, H.;
729 Covaci, A. The stability of illicit drugs and metabolites in wastewater, an important
730 issue for sewage epidemiology? *J. Hazard. Mater.* **2012**, *239–240*, 19–23.
- 731 (8) Senta, I.; Krizman, I.; Ahel, M.; Terzic, S. Assessment of stability of drug biomarkers
732 in municipal wastewater as a factor influencing the estimation of drug consumption
733 using sewage epidemiology. *Sci. Total Environ.* **2014**, *487*, 659–665.
- 734 (9) Baker, D. R.; Očenášková, V.; Kvicálová, M.; Kasprzyk-Hordern, B. Drugs of abuse
735 in wastewater and suspended particulate matter - Further developments in sewage
736 epidemiology. *Environ. Int.* **2012**, *48*, 28–38.
- 737 (10) Baker, D. R.; Kasprzyk-Hordern, B. Critical evaluation of methodology commonly
738 used in sample collection, storage and preparation for the analysis of pharmaceuticals
739 and illicit drugs in surface water and wastewater by solid phase extraction and liquid
740 chromatography-mass spectrometry. *J. Chromatogr. A* **2011**, *1218* (44), 8036–8059.
- 741 (11) Polesel, F.; Andersen, H. R.; Trapp, S.; Plósz, B. G. Removal of Antibiotics in
742 Biological Wastewater Treatment Systems □ A Critical Assessment Using the
743 Activated Sludge Modeling Framework for Xenobiotics (ASM-X). *Environ. Sci.*
744 *Technol.* **2016**, *50* (19), 10316–10334.
- 745 (12) Ramin, P.; Brock, A. L.; Polesel, F.; Causanilles, A.; Emke, E.; de Voogt, P.; Plósz,
746 B. G. Transformation and sorption of illicit drug biomarkers in sewer systems:
747 understanding the role of suspended solids in raw wastewater. *Environ. Sci. Technol.*
748 **2016**, *50* (24), 13397–13408.
- 749 (13) Thai, P. K.; Jiang, G.; Gernjak, W.; Yuan, Z.; Lai, F. Y.; Mueller, J. F. Effects of

- 750 sewer conditions on the degradation of selected illicit drug residues in wastewater.
751 *Water Res.* **2014**, *48*, 538–547.
- 752 (14) McCall, A.-K.; Scheidegger, A.; Madry, M. M.; Steuer, A. E.; Weissbrodt, D. G.;
753 Vanrolleghem, P. A.; Kraemer, T.; Morgenroth, E.; Ort, C. Influence of different
754 sewer biofilms on transformation rates of drugs. *Environ. Sci. Technol.* **2016**, *50* (24),
755 13351–13360.
- 756 (15) Ort, C.; Gujer, W. Sorption and high dynamics of micropollutants in sewers. *Water*
757 *Sci. Technol.* **2008**, *57* (11), 1791–1797.
- 758 (16) Plósz, B. G.; Reid, M. J.; Borup, M.; Langford, K. H.; Thomas, K. V.
759 Biotransformation kinetics and sorption of cocaine and its metabolites and the factors
760 influencing their estimation in wastewater. *Water Res.* **2013**, *47* (7), 2129–2140.
- 761 (17) Bisceglia, K. J.; Lippa, K. a. Stability of cocaine and its metabolites in municipal
762 wastewater - the case for using metabolite consolidation to monitor cocaine
763 utilization. *Environ. Sci. Pollut. Res.* **2014**, *21* (516), 4453–4460.
- 764 (18) Jiang, F.; Leung, D. H.-W. W.; Li, S.; Chen, G.-H. H.; Okabe, S.; van Loosdrecht, M.
765 C. M. A biofilm model for prediction of pollutant transformation in sewers. *Water*
766 *Res.* **2009**, *43* (13), 3187–3198.
- 767 (19) Schwarzenbach, R. P.; Gschwend, P. M.; Imboden, D. M. *Environmental Organic*
768 *Chemistry*; Wiley Interscience: Hoboken, NJ, 2003.
- 769 (20) Wicke, D.; Böckelmann, U.; Reemtsma, T. Experimental and modeling approach to
770 study sorption of dissolved hydrophobic organic contaminants to microbial biofilms.
771 *Water Res.* **2007**, *41* (10), 2202–2210.
- 772 (21) Torresi, E.; Polesel, F.; Bester, K.; Christensson, M.; Smets, B. F.; Trapp, S.;
773 Andersen, H. R.; Plósz, B. G. Diffusion and sorption of organic micropollutants in
774 biofilms with varying thicknesses. *Water Res.* **2017**.
- 775 (22) Huisman, J. L.; Gujer, W. Modelling wastewater transformation in sewers based on
776 ASM3. *Water Sci. Technol.* **2002**, *45* (6), 51–60.
- 777 (23) EMCDDA. *European Drug Report*; 2017.
- 778 (24) Boerner, U.; Abbott, S.; Roe, R. L. The Metabolism of Morphine and Heroin in Man.
779 *Drug Metab. Rev.* **1975**, *4* (1), 39–73.
- 780 (25) Rochex, A.; Godon, J.; Bernet, N.; Escudie, R. Role of shear stress on composition ,
781 diversity and dynamics of biofilm bacterial communities. *Water Res.* **2008**, *42*, 4915–
782 4922.
- 783 (26) Oms, C.; Gromaire, M. C.; Saad, M.; Milisic, V.; Chebbo, G.; Gromaire, M. C.; Saad,
784 M.; Milisic, V.; Bed, G. C. Bed shear stress evaluation in combined sewers. *Urban*
785 *Water J.* **2008**, *5* (3), 219–229.
- 786 (27) APHA. *Standard methods for the examination of water and wastewater. American*
787 *Public Health Association*, 19th ed.; Washington, D.C, 1995.
- 788 (28) Bijlsma, L.; Emke, E.; Hernández, F.; de Voogt, P. Performance of the linear ion trap
789 Orbitrap mass analyzer for qualitative and quantitative analysis of drugs of abuse and
790 relevant metabolites in sewage water. *Anal. Chim. Acta* **2013**, *768* (1), 102–110.
- 791 (29) Horn, H.; Hempel, D. C. Modeling mass transfer and substrate utilization in the

- 792 boundary layer of biofilm systems. *Water Sci. Technol.* **1998**, *37* (4–5), 139–147.
- 793 (30) Othmer, D. F.; Thakar, M. S. Correlating Diffusion Coefficients in Liquids. *Ind. Eng.*
794 *Chem.* **1953**, *45* (3), 589–593.
- 795 (31) Hayduk, W.; Laudie, H. Prediction of diffusion coefficients for nonelectrolytes in
796 dilute aqueous solutions. *AIChE J.* **1974**, *20* (3), 611–615.
- 797 (32) Guimerà, X.; Dorado, A. D.; Bonsfills, A.; Gabriel, G.; Gabriel, D.; Gamisans, X.
798 Dynamic characterization of external and internal mass transport in heterotrophic
799 biofilms from microsensors measurements. *Water Res.* **2016**, *102*, 551–560.
- 800 (33) Wanner, O.; Eberl, H. J.; Morgenroth, E.; Noguera, D. R.; Picioreanu, C.; Rittmann,
801 B. E.; van Loosdrecht, M. C. . *Mathematical modeling of biofilms*; 2006.
- 802 (34) Recktenwald, A.; Lücke, M.; Müller, H. W. Taylor vortex formation in axial through-
803 flow: Linear and weakly nonlinear analysis. *Phys. Rev. E* **1993**, *48* (6), 4444–4454.
- 804 (35) Castiglioni, S.; Zuccato, E.; Fanelli, R. *Illicit Drugs in the Environment: Occurrence,*
805 *Analysis, and Fate Using Mass Spectrometry*; JohnWiley & Sons, Inc, 2011.
- 806 (36) Laloy, E.; Vrugt, J. a. High-dimensional posterior exploration of hydrologic models
807 using multiple-try DREAM(ZS) and high-performance computing. *Water Resour.*
808 *Res.* **2012**, *48* (1), 1–18.
- 809 (37) Ramin, P.; Valverde-Pérez, B.; Polesel, F.; Locatelli, L.; Plósz, B. G. A systematic
810 model identification method for chemical transformation pathways – the case of
811 heroin biomarkers in wastewater. *Sci. Report, Accept. with Revis.* **2017**.
- 812 (38) Vangsgaard, A. K.; Mauricio-Iglesias, M.; Gernaey, K. V.; Smets, B. F.; Sin, G.
813 Sensitivity analysis of autotrophic N removal by a granule based bioreactor: Influence
814 of mass transfer versus microbial kinetics. *Bioresour. Technol.* **2012**, *123*, 230–241.
- 815 (39) Sin, G.; Gernaey, K. V.; Neumann, M. B.; van Loosdrecht, M. C. M.; Gujer, W.
816 Uncertainty analysis in WWTP model applications: A critical discussion using an
817 example from design. *Water Res.* **2009**, *43* (11), 2894–2906.
- 818 (40) Rosa Boleda, M.; Huerta-Fontela, M.; Ventura, F.; Galceran, M. T. Evaluation of the
819 presence of drugs of abuse in tap waters. *Chemosphere* **2011**, *84* (11), 1601–1607.
- 820 (41) Plósz, B. G.; Langford, K. H.; Thomas, K. V. An activated sludge modeling
821 framework for xenobiotic trace chemicals (ASM-X): Assessment of diclofenac and
822 carbamazepine. *Biotechnol. Bioeng.* **2012**, *109* (11), 2757–2769.
- 823 (42) Torresi, E.; Fowler, J. S.; Polesel, F.; Bester, K.; Andersen, H. R.; Smets, B. F.; Plósz,
824 B. G.; Christensson, M. Biofilm thickness influences biodiversity in nitrifying
825 MBBRs – Implications on micropollutant removal. *Environ. Sci. Technol.* **2016**, *50*
826 (17), 9279–9288.
- 827 (43) Sathyamoorthy, S.; Chandran, K.; Ramsburg, C. A. Biodegradation and Cometabolic
828 Modeling of Selected Beta Blockers during Ammonia Oxidation. *Environ. Sci.*
829 *Technol.* **2013**, *47*, 12835–12843.
- 830 (44) Bisceglia, K. J.; Roberts, A. L.; Lippa, K. A. A hydrolysis procedure for the analysis
831 of total cocaine residues in wastewater. *Anal. Bioanal. Chem.* **2012**, *402*, 1277–1287.
- 832 (45) Bisceglia, K. J. K.; Lippa, K. a. Stability of cocaine and its metabolites in municipal
833 wastewater - the case for using metabolite consolidation to monitor cocaine

- 834 utilization. *Environ. Sci. Pollut. Res.* **2014**, *21* (6), 4453–4460.
- 835 (46) Stefanidou, M.; Athanasis, S.; Spiliopoulou, C.; Dona, A.; Maravelias, C.
836 Biomarkers of opiate use. *Int. J. Clin. Pract.* **2010**, *64* (12), 1712–1718.
- 837 (47) Castiglioni, S.; Zuccato, E.; Crisci, E.; Chiabrando, C.; Fanelli, R.; Bagnati, R.
838 Identification and measurement of illicit drugs and their metabolites in urban
839 wastewater by liquid chromatography-tandem mass spectrometry. *Anal. Chem.* **2006**,
840 *78* (24), 8421–8429.
- 841 (48) ACD/I-Lab 2.0 Prediction Software by Advanced Chemistry Development Inc.
842 (ACD/Labs).
- 843 (49) Mccall, A.; Palmitessa, R.; Blumensaat, F.; Morgenroth, E.; Ort, C. Modeling in-
844 sewer transformations at catchment scale – Implications on drug consumption
845 estimates in wastewater-based epidemiology. *Water Res.* **2017**.
- 846 (50) Ramin, P. Modelling Illicit Drug Fate in Sewers for Wastewater-Based
847 Epidemiology, PhD Thesis, Technical University of Denmark, 2016.
- 848
- 849

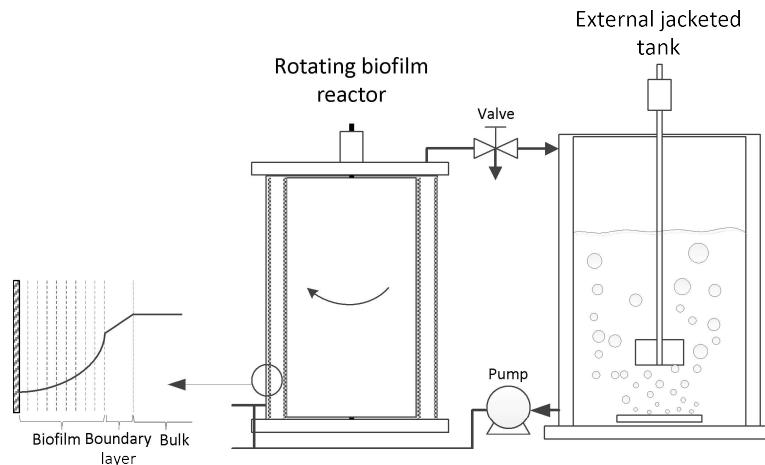
850 **Table 1.** Model state variables and parameters

Symbol	Definition	Units	Values
A_b	Biofilm area	m^2	4.10^{-3}
C_R	Concentration of drug biomarkers in reactor	$g L^{-1}$	
C_b	Concentration of drug biomarkers inside biofilm	$g L^{-1}$	
C_T	Concentration of drug biomarkers in external tank bulk phase	$g L^{-1}$	
C_{Tw}	Concentration of drug biomarkers sorbed onto external tank wall	$g L^{-1}$	
d	Gap between rotating drum and stationary cylinder (R_2-R_1)	m	0.012
d_R	Reactor Characteristic length ($2d$)		0.024
D	Diffusion coefficient of the soluble compounds into the biofilm	$m^2 d^{-1}$	Table S2
D_w	Diffusion coefficient of the soluble compounds in water	$m^2 d^{-1}$	Table S2
f	Dimensionless effective diffusivity	-	ae:0.68 an:0.38
j_b	Flux of compounds between bulk phase and the biofilm	$g m^{-2} d^{-1}$	
k_b	Mass transfer coefficient between bulk phase and the biofilm	$m d^{-1}$	
$k_{des,w}$	Desorption from reactor wall	d^{-1}	100
K_{dw}	Reactor wall–liquid partition coefficient	$m^3 m^{-2}$	Ramin et al. ¹²
K_d	Suspended Solid–liquid partition coefficient	$L gTSS^{-1}$	Ramin et al. ¹²
K_{df}	Suspended biofilm–liquid partition coefficient	$L gTSS^{-1}$	Table S4
k_{abio}	Abiotic transformation rate constant	d^{-1}	Ramin et al. ¹²
k_{bio}	TSS-normalized biotransformation rate constant	$L gTSS^{-1} d^{-1}$	Ramin et al. ¹²
k_f	Sewer biofilm biotransformation rate (eq. 9)	d^{-1}	Figure S11
k_{biof}	TSS-normalized Sewer biofilm biotransformation rate	$L gTSS^{-1} d^{-1}$	Table S4
k'_{biof}	Area-to-volume-normalized Sewer biofilm biotransformation rate	$m^3 m^{-2} d^{-1}$	Table S4
L_b	Concentration boundary layer	m	23.10^{-6}
M	Biomarker molecular weight	$g mol^{-1}$	Table S2
O	Observed (measured) values		
P	Predicted (simulated) values		
$Q_{in,R}$	Reactor inflow	$m^3 d^{-1}$	4.10^{-3}
$Q_{out,R}$	Reactor outflow	$m^3 d^{-1}$	4.10^{-3}
$Q_{in,T}$	External tank inflow	$m^3 d^{-1}$	4.10^{-3}
$Q_{out,T}$	External tank outflow	$m^3 d^{-1}$	4.10^{-3}
r_R	Reaction rate in reactor	$g L d^{-1}$	
r_b	Reaction rate in side biofilm	$g L d^{-1}$	
r_T	Reaction rate in external tank	$g L d^{-1}$	
R_1	Reactor inner radius (outer radius of rotating drum)	m	0.045
R_2	Reactor outer radius (inner radius of stationary cylinder)	m	0.057
V_R	Total reactor volume	m^3	$9.61.10^{-4}$
\bar{u}	Average axial velocity inside reactor (a continuous operation; b: batch experiment)	$m s^{-1}$	a: $0.12.10^{-4}$ a: $2.89.10^{-4}$
V_b	Biofilm volume	m^3	ae: $1.25.10^{-4}$ an: $1.71.10^{-4}$
V_T	Bulk volume in external volume	m^3	Figure S2
V_l	Molar volume	$cm^3 g mole^{-1}$	Table S2
X_{SS}	Concentration of suspended solids	$gTSS L$	Table S3
ΔZ	Discretization distance inside biofilm for spatial discretization of partial differential equations	m	ae: $9.3 10^{-6}$ an: $12.8 10^{-6}$
μ_w	Dynamic viscosity of water (at $\sim 17^\circ C$)	$kg m^{-1} s^{-1}$	$1.07 10^{-3}$
ν	Kinematic viscosity of water (at $\sim 17^\circ C$)	$m^2 s^{-1}$	$1.07 10^{-6}$
σ_w	Wet-surface-to-volume ratio	$m^2 m^{-3}$	Figure S2
Ω	Angular velocity of rotating drum	$rad d^{-1}$	2.09

851

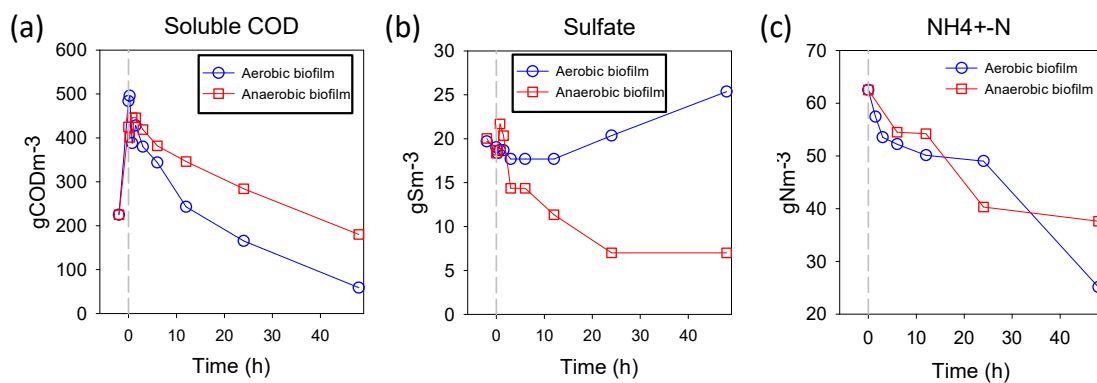
852

853



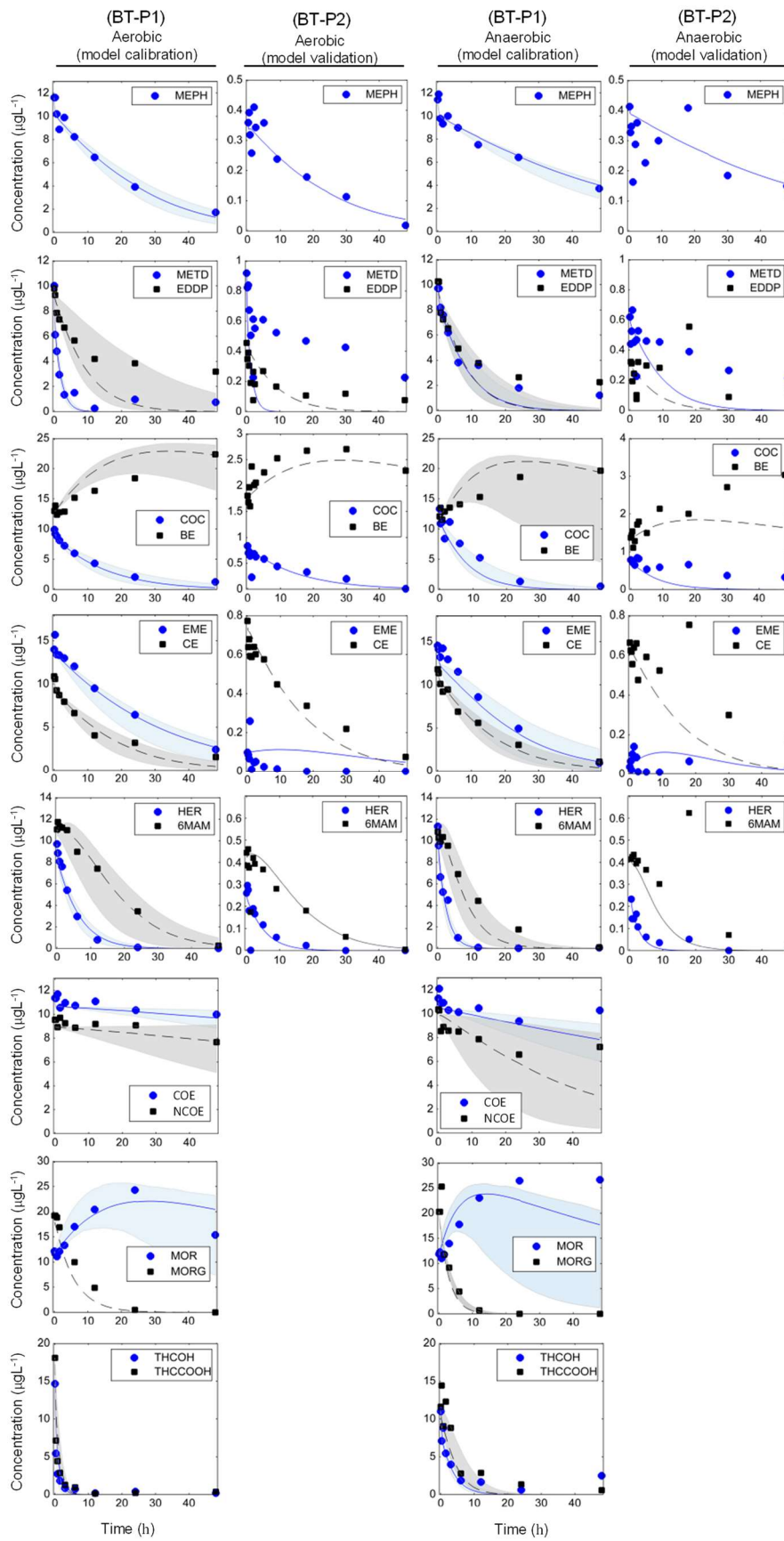
854 **Figure 1.** Configuration of rotating biofilm reactor (on the left) connected to an external tank (on
855 the right) during batch experiments. The samples were taken from the outlet of the biofilm reac-
856 tor, on the top valve. Anaerobic or aerobic conditions were maintained in the external tank by
857 sparging air or nitrogen, respectively, from a diffuser placed at the bottom of the tank. A typical
858 drug concentration profile inside the biofilm is also presented.
859

860

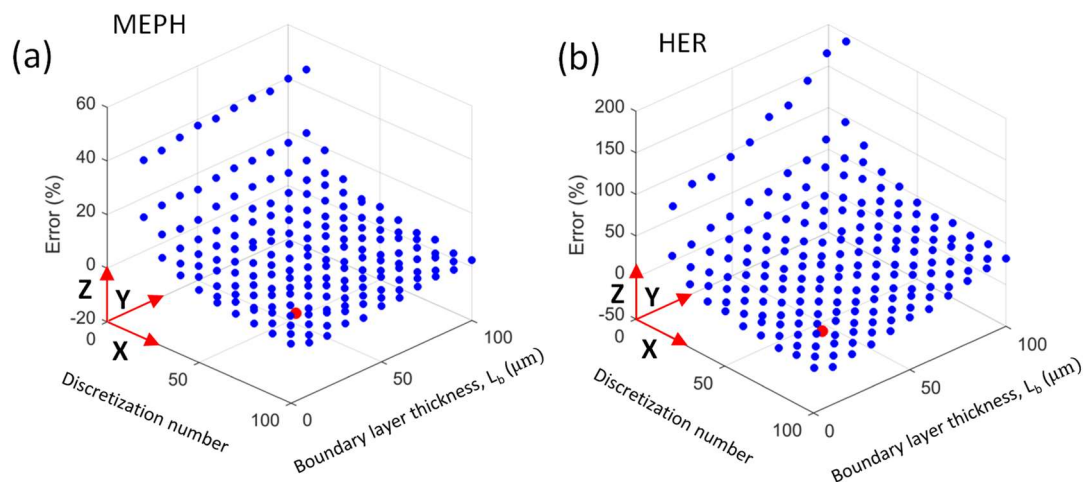


861 **Figure 2.** Soluble COD, sulfate and ammonium concentrations measured during BT-P1 ex-
862 periments under aerobic and anaerobic conditions. Measurements before t=0 refer to samples
863 taken prior to the spiking of standards, and the subsequent increase of soluble COD concen-
864 tration at t=0 should be associated with the addition of MeOH resulting from spiking of
865 biomarkers mixture. Lines connecting data points are based on simple linear interpolation to
866 show the trends.

867



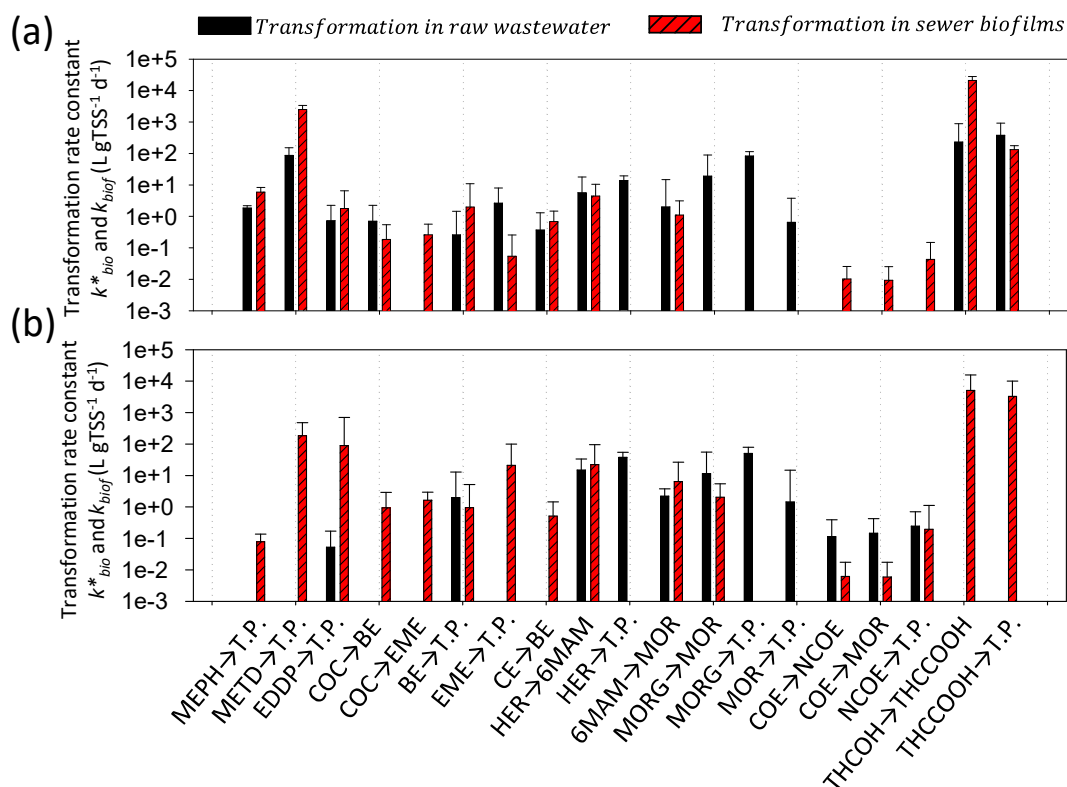
869 **Figure 3.** Experimental data and simulation results for biomarker transformations in sewer
870 biofilm under aerobic and anaerobic conditions. Results are related to model calibration us-
871 ing BT-P1 experimental data and model validation using BT-P2 experimental data. THC
872 data is presented in (SI, Figure S10). Markers are measured data and lines are simulation
873 results. The shaded areas reflect 95% credibility interval of model prediction.



874

875 **Figure 4.** The impact of discretization number (number of discretization layers considered
 876 for numerical integration in biofilm) and boundary layer thickness on estimation of aerobic
 877 transformation rate, k_f (d^{-1}), for MEPH and HER. 190 scenarios were considered for each
 878 chemical. The parameter estimate at each scenario was compared with the reference scenario
 879 for each chemical. The reference scenario contained 100 layers using the accurate estimation
 880 of boundary layer thickness, i.e. $30 \mu\text{m}$ for MEPH and $20 \mu\text{m}$ for HER. Blue dots are the
 881 data resulted from scenarios and red dots correspond to the values chosen in this study (i.e.
 882 80 discretization number and $23 \mu\text{m}$ boundary layer thickness). Considering this choice re-
 883 sulted in an acceptable error i.e. 0.4% for MEPH and 2% for HER.

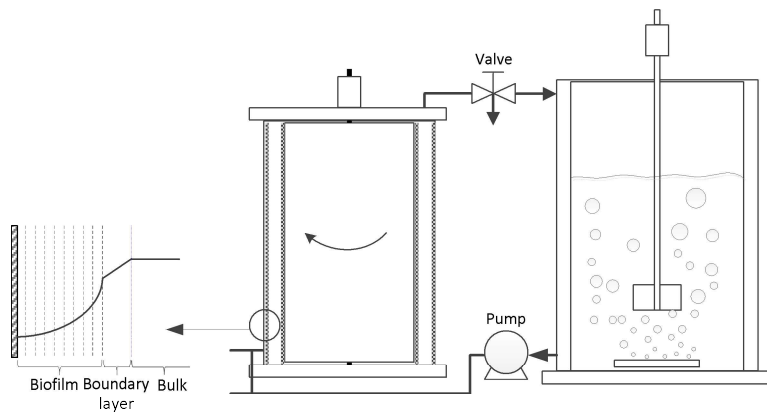
884



885

886 **Figure 5.** Comparing the biotransformation of drug biomarkers in raw wastewater and bio-
 887 transformation in sewer biofilms under aerobic (a), and anaerobic (b) conditions. For this
 888 comparison, TSS-normalized transformation rate constants in raw wastewater k_{bio} ($L\ gTSS^{-1}\ d^{-1}$)
 889 reported in Ramin et al.¹² are compared with sewer biofilm-mediated transformation
 890 rate constants, k_{biof} ($L\ gTSS^{-1}\ d^{-1}$), from this study. Error bars identify the upper bound of the
 891 95% credibility interval of estimated parameters.

892 TOC/graphical abstract



893